Reorganization of polar cap patches through shears in the background plasma convection

K. Hosokawa,[1] J.-P. St-Maurice,[2] G. J. Sofko,[2] K. Shiokawa,[3] Y. Otsuka,[3] and T. Ogawa[4]

[1]   On the night of December 20, 2006, 630 nm airglow images obtained by an all-sky camera at Resolute Bay, Canada (74.73°N, 265.07°E; altitude adjusted corrected geomagnetic (AACGM) latitude 82.9°) showed the passage of successive polar cap patches. Shortly after convection came to a temporary halt, one of the patches was reorganized into two substructures in approximately 8 min. The two-dimensional background ionospheric convection pattern measured using the newly deployed PolarDARN radar at Rankin Inlet (62.82°N, 93.11°W; AACGM latitude 72.96°) showed that a velocity shear of approximately $120 \text{ m s}^{-1}/340 \text{ km}$ suddenly appeared in the vicinity of the patch at the time of reorganization. A qualitative analysis of the relationship between the magnitude of the velocity shear and the distance between the divided patches indicates that the shear in the background plasma convection velocity significantly contributed to the reorganization of the patch. This shear structure appeared soon after a southward turning of the interplanetary magnetic field (IMF) and was probably associated with the reconfiguration of the convection pattern from a pre-existing northward-oriented IMF pattern to a southward-oriented one. The present observations indicate that the reconfiguration/deformation of patches because of a shear in the background convection field, especially reorganization of patches into smaller substructures, may play an important role in the rapid structuring of patches.

1.   Introduction

[2]   Polar cap patches are high-plasma density regions that often appear in the polar cap *F* region ionosphere. They are thought to be generated in the vicinity of the dayside cusp region when the interplanetary magnetic field (IMF) is directed southward. Once they are generated on the dayside, they are transported toward the nightside across the central polar cap along the streamline of the higher latitude portion of the twin-cell convection pattern [*Crowley*, 1996; *Hosokawa et al.*, 2006; 2009b]. The horizontal extent of patches typically ranges from 100 km to 1000 km, and the plasma density within these patches is often up to 10 times higher than that in neighboring regions [*Weber et al.*, 1984].

[3]   It is relatively well established that a "tongue of ionization (TOI)" is a source of patches [*Sojka et al.*, 1993]. The TOI is a region with dense daytime thermal plasma that is drawn from a sunlit sub-cusp region into the polar cap through the cusp region [*Knudsen*, 1974]. There are several proposed processes through which daytime dense plasmas detach from a continuous TOI as discrete patches, such as the IMF-controlled reorientation of a cusp inflow region [*Decker et al.*, 1994; *Milan et al.*, 2002], convection jets [*Rodger et al.*, 1994], in situ plasma reduction under an intense electric field [*Valladares et al.*, 1994; *Ogawa et al.*, 2001], polar cap expansion and contraction [*Anderson et al.*, 1988], an expansion of the polar cap convection pattern by pulsed reconnection [*Lockwood and Carlson*, 1992; *Carlson et al.*, 2006], and bursty plasma transport from the subauroral latitudes [*Moen et al.*, 2006]. Recent coordinated measurements of ionospheric plasma parameters around the dayside cusp have provided evidence for all the mechanisms introduced above, although it is still unknown which of these processes is the dominant one, if there is a dominant one. An important point to remember is that all the above mentioned mechanisms are based on temporal variations associated with the plasma convection pattern near the cusp region, which causes patches to detach from a TOI.

[4]   Patches are usually transported over very long distances across the central polar cap region before they convect into the nightside auroral zone. It is now believed that some patches distort into latitudinally confined "boundary blobs" that extend over many degrees of longitude when they enter the sunward convection region of a nightside

[1]Department of Information and Communication Engineering, University of Electro-Communications, Tokyo, Japan.
[2]Institute for Space and Atmospheric Studies, Department of Physics and Engineering Physics, University of Saskatchewan, Saskatoon, Saskatchewan, Canada.
[3]Solar-Terrestrial Environment Laboratory, Nagoya University, Nagoya, Japan.
[4]National Institute of Information and Communications Technology, Tokyo, Japan.

auroral region [e.g., *de la Beaujardiere and Heelis*, 1984; *Tsunoda*, 1988]. This reconfiguration process was first modeled by *Robinson et al.* [1985] by using the two-cell convection pattern of *Heelis et al.* [1982]. In their simulation, patches straddle convection streamlines that circulate in both convection cells (i.e., dawn cell and dusk cell). As a result, a substantial elongation of the patches in the longitudinal direction occurs because a portion of the patch plasma is transported westward along the sunward flow in the dusk convection cell, and the remainder is captured by the eastward flow in the dawn convection cell. This deformation process of a patch into a boundary blob is essentially due to a spatial shear in the convection streamline.

[5] As mentioned above, the reconfiguration of large-scale structures, such as "TOI into patches" and "patches into boundary blobs," is closely associated with the temporal and spatial variations in the background plasma convection pattern. Such processes have been studied extensively by carrying out several ionospheric measurements at the latitudes of the cusp and nightside auroral regions. In contrast, however, the deformation process of patches during their travel within the central polar cap region has not been investigated thoroughly by measurements. A major obstacle to conducting such studies has been the limited number of instruments that can observe two-dimensional background plasma convection patterns in the central polar cap region. However, the recent deployment of the PolarDARN coherent radars, which scan the central polar cap region, allows us to monitor the background plasma convection pattern in the vicinity of patches traveling through the central polar cap region. In this paper, we report on an event during which a patch was reorganized into two substructures when the background plasma convection field became spatially inhomogeneous in the vicinity of the original patch. During the event, the patches were observed with an all-sky airglow imager at Resolute Bay, while the background convection pattern was monitored with the PolarDARN radar at Rankin Inlet.

2. Instrumentation

[6] The all-sky airglow imager at Resolute Bay (74.73°N, 265.07°E; AACGM latitude 82.9°) has been operational since January 2005 [*Hosokawa et al.*, 2006] as part of Optical Mesosphere Thermosphere Imagers (OMTIs) [*Shiokawa et al.*, 1999]. The imager has a number of optical filters for various wavelengths and bandwidths, such as 557.7 nm, 630.0 nm, 777.4 nm, the Na line and the OH band; this enables us to study various upper atmospheric phenomena occurring in the polar cap region, such as polar cap patches [*Hosokawa et al.*, 2006, 2009a, 2009b], TOI [*Hosokawa et al.*, 2009c], polar cap aurora [*Koustov et al.*, 2008], and gravity waves at mesospheric heights [*Suzuki et al.*, 2009]. In the present analysis, all-sky airglow images at a wavelength of 630.0 nm (OI, emission altitude ranging from 200 to 300 km), which were obtained every 2 min with an exposure time of 30 s, were employed for observing the two-dimensional behavior of polar cap patches. Background continuum emission from the sky was sampled every 20 min at a wavelength of 572.5 nm and was used to derive the absolute intensity of the airglow lines [*Shiokawa et al.*, 2000, 2009].

[7] The PolarDARN Rankin Inlet radar (62.82°N, 93.11°W; AACGM latitude 72.96°), which forms a part of the international SuperDARN network [*Greenwald et al.*, 1995; *Chisham et al.*, 2007], has been operational since 2006. The radar has been used extensively for studying various phenomena occurring in the polar cap region, for which it has a favorable viewing geometry. The Rankin Inlet radar shares a large common field of view (FOV) with the all-sky imager at Resolute Bay. In particular, beam 5 of the Rankin Inlet radar overlooks the zenith of the all-sky imager at Resolute Bay. During the interval presented in this paper, the radar was operating in fast normal-scan mode. In the current version of this mode, the radar scans through 16 beams every minute, with an integration time of 3 s for each beam, which are binned into 100 range gates (separation between the gates is 45 km). The operating frequency stayed between 12.2 and 12.5 MHz.

3. Observations

[8] Figure 1 shows the IMF B_y and B_z components and the solar wind velocity during a 2 h interval from 2130 to 2330 UT on December 20, 2006. The all-sky imager at Resolute Bay observed a reorganization of the spatial structure of polar cap patch in the middle of this time interval. This set of solar wind data was obtained by the MAG and SWEPAM instruments onboard the ACE spacecraft located far upstream of the Earth ($X_{GSM} = 225.5 \, R_e$). A solar wind velocity of approximately 700 km s^{-1} was measured by ACE (Figure 1c) throughout the interval, implying a delay of 38 min between the observed IMF feature at the spacecraft location and its incidence on the dayside magnetopause. Additional 2 min were added to account for the propagation of Alfvén waves from the subsolar magnetopause to the dayside polar cap ionosphere. These calculations were carried out by the technique proposed by *Khan and Cowley* [1999]. In Figure 1, the time series of the IMF and solar wind data were shifted accordingly. The error in the estimation of the time delay can vary between 5 and 20 min depending on the method used [*Ridley*, 2000]. Since timing is crucial for the following discussion, we double checked the accuracy of the estimated delay time by comparing the delayed IMF data with the SuperDARN convection maps. That is, we examined timing of the change of sign in the IMF B_z and the variation of the dayside convection strength. As a result, the error in the time delay was found to be less than 2 min, which suggests that the time delay of 40 min estimated above is almost accurate. Except for an interval of northward IMF from 2205 to 2230 UT, the B_z component of the IMF (Figure 1b) was mostly negative at around −5 nT, indicating favorable conditions for the generation of polar patches near the cusp region and subsequent delivery into the central polar cap region [*Crowley*, 1996]. The B_y component of the IMF (Figure 1a) changed its orientation more frequently. However, it was mostly positive at around 5 nT between 2200 and 2250 UT.

[9] Figure 2 shows a sequence of the 630.0 nm all-sky airglow images picked at 4 min intervals from 2202 to 2258 UT. The original all-sky images have been cut at an 80° zenith angle and were converted into altitude adjusted corrected geomagnetic (AACGM) coordinates [*Baker and*
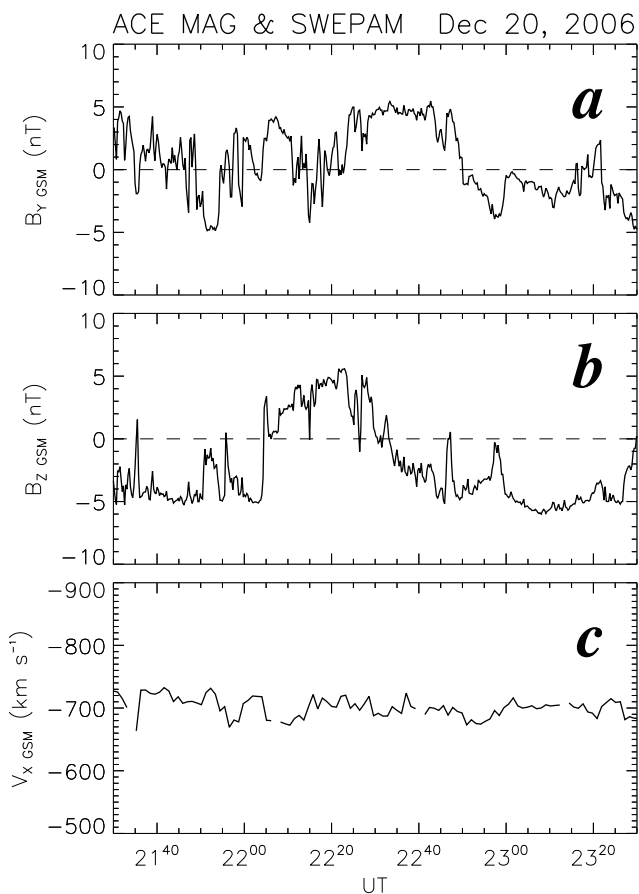
ACE MAG & SWEPAM   Dec 20, 2006

Figure 1. Solar wind velocity and IMF components measured between 2130 and 2330 UT on December 20, 2006 by the SWEPAM and MAG instruments on board the ACE spacecraft. The time series are time shifted by 40 min to allow for solar wind propagation delay.

Wing, 1989], and then mapped onto magnetic latitude/MLT coordinates. It is impossible to determine the emission height of patches only from a single-optical observation. *Lorentzen et al.* [2004] estimated the altitude of patches using triangulation between two ground-based optical stations. During the events they investigated that the patch was found to have an altitude of around 300 km. In this paper, we assume an emission altitude of 250 km for mapping the all-sky images onto the AACGM coordinates. Magnetic noon is shown to the top, and the dashed circle represents a magnetic latitude of 80°. Here, the absolute optical intensities are scaled in units of Rayleigh. Throughout the interval presented, the dayside part of the FOV was illuminated by the sun under the horizon, since the terminator at the F region height is substantially offset from the ground level terminator. At 2202 UT (image a), patch A was observed in the eastern part of the FOV, and patch B was emerging from the bright area on the dayside. Subsequently, patch A drifted anti-sunward and almost moved out of the FOV at around 2218 UT (image e). In turn, patch B reached the center of the FOV at 2218 UT. After this image, patch B did not move in any specific direction and was almost stationary around the zenith for approximately 8 min (2218–2226 UT: images e–g), which implies that background convection ceased at

this time. We will discuss this point further in the later part of this section. At 2230 UT (image h), a gap appeared in the central part of patch B. Subsequently, the width of the gap increased, and finally, patch B split into two substructures at around 2238 UT (image j). After the splitting, the two substructures (we denote these two as patches B1 and B2) drifted duskward and eventually moved almost out of the FOV by 2258 UT (image o).

[10] Before moving on, it should be noted that the phenomenon which we call "splitting" does not exactly mean "complete splitting" of patch. This is primarily because there is no evidence that the 630.0 nm optical intensity (i.e., electron density) was zero at the gap between patches B1 and B2 since the imager has a minimum threshold for detectable optical emission intensity. Thus, patch B did not split into two individual parts completely but just had two substructures inside it. Hereinafter, we call this phenomenon as "reorganization" of the spatial structure of patch plasma rather than "splitting" to make this point clearer.

[11] In order to investigate the factor that caused the reorganization of patch B, we examined the background plasma convection pattern in the vicinity of patch B, as obtained by the PolarDARN radar at Rankin Inlet. Figure 3 shows 630.0 nm airglow images recorded from 2226 to 2238 UT, during which the reorganization occurred. To indicate the slight enhancement in airglow caused by the patch, here, the airglow distribution is shown as a percentage deviation from a 1 h running average [*Hosokawa et al.*, 2006; 2009a]. The background subtraction process is as follows: (1) calculate an average image for a 1 h temporal window. For example, when we derive the average image at 2230 UT, we employ 30 images (obtained every 2 min) from 2200 to 2300 UT, (2) subtract the average image from the current image. The duration of the temporal window employed in the averaging process is 1 h, which is well longer than the duration of the patch. Thus, this background subtraction process does not cause artificial change of the spatial structure of the patch shown in Figure 3. In each subset of Figure 3, the two-dimensional plasma convection vectors and potential contours, as derived by the map-potential technique proposed by *Ruohoniemi and Baker* [1998], were superimposed on the all-sky images for comparison. We used the data from all the SuperDARN radars in the Northern Hemisphere to construct these convection patterns. However, most of the vectors within the FOV of the all-sky imager were obtained by the Polar-DARN radar at Rankin Inlet.

[12] Before the reorganization of the patch occurred (images a, d and b, e), the convection velocity around patch B was very small (less than 100 m s^{-1}). As mentioned above, patch B was almost stationary around the zenith between 2218 and 2226 UT. This stagnation of patch B was consistent with the very slow plasma convection that occurred in its vicinity. At 2230 UT (images c, f), the plasma convection velocity within the FOV enhanced significantly; the flow direction near the patch was almost duskward. This was the time at which the reorganization of patch B commenced. It is interesting to note that the convection speed was clearly higher in the equatorward half of patch B (left-hand side in Figures 3g and 3h; this part of patch B corresponded to patch B1 after the reorganiza-
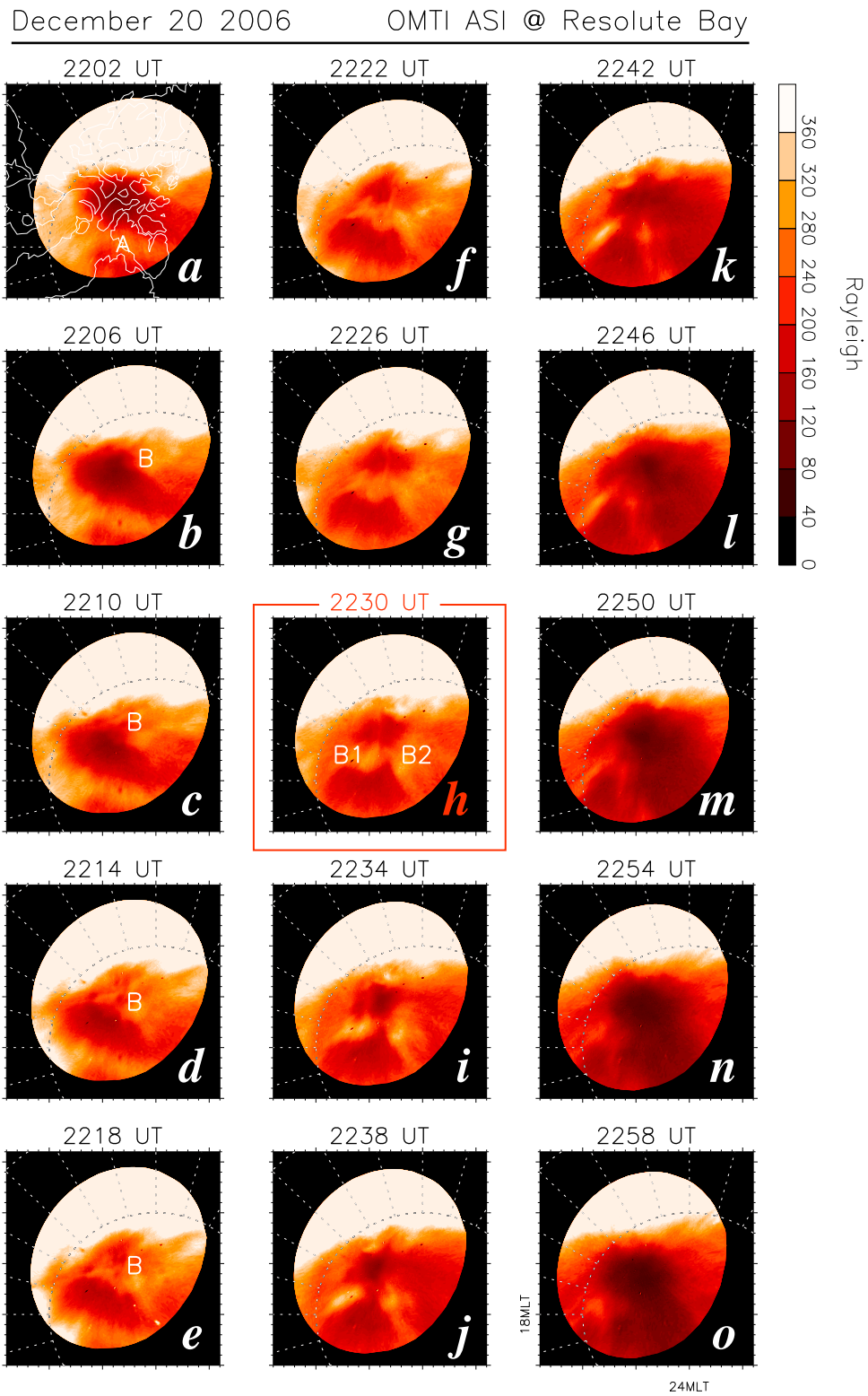
Figure 2. Sequence of 630.0 nm airglow images obtained at 4 min intervals from 2202 to 2258 UT. The images are shown in magnetic latitude/MLT coordinates, and the absolute airglow intensity is scaled in units of Rayleigh. Magnetic noon is at the top, and the dashed circle represents a magnetic latitude of 80°. The approximate time of reorganization of patch is highlighted by a red rectangle.
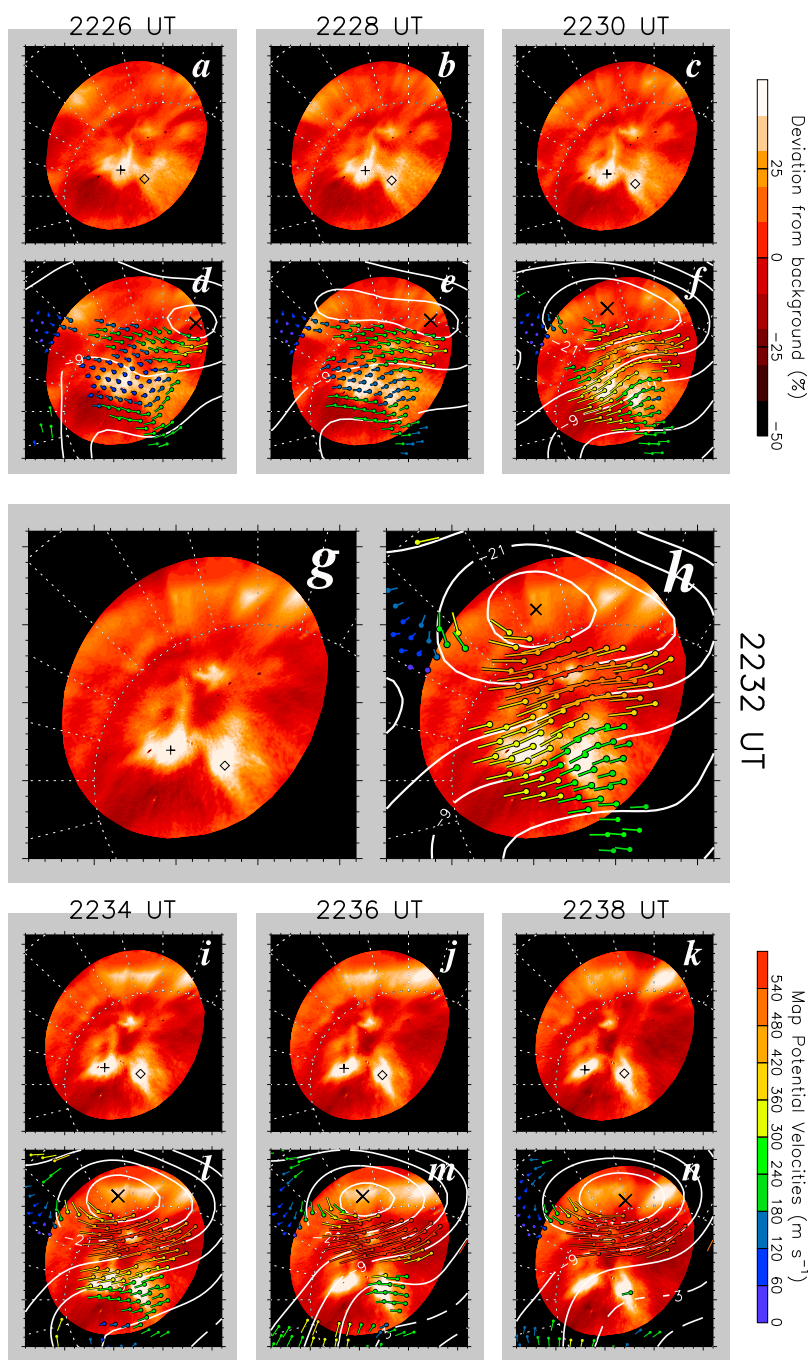
Figure 3. The 630.0 nm airglow images obtained at 2 min intervals from 2226 to 2238 UT. In some of the images (Figures 3d, 3e, 3f, 3h, 3l, 3m, and 3n), the contours of electrostatic potential and vectors of two-dimensional plasma drift derived by the map-potential technique [*Ruohoniemi and Baker*, 1998] are overplotted.

tion). This signature was seen when the reorganization was in progress (images f, h and l), but was most clearly seen at 2232 UT (image h). At 2230 UT, the convection speed in the equatorward half of patch B was approximately 330 m s^{-1}, while that in the poleward half was approximately 250 m s^{-1}. This difference in the convection speed of approximately 80 m s^{-1} gradually led to the detaching of the equatorward half of patch B from its main body, and finally, patch B had two substructures patches B1 and B2. After 2236 UT, radar backscatter echoes associated with the patch disappeared;

thus, we could not directly monitor the convection pattern around patches B1 and B2.

[13]   Here, we briefly mention the accuracy of the convection pattern estimation using the map-potential technique. The map-potential technique employs the IMF-dependent convection model in the region where the amount of the radar backscatter echoes is not sufficient for the spherical harmonics fitting. The PolarDARN Rankin Inlet radar obtained lots of backscatters in the central part of the FOV of the imager, which suggests that the derived con-
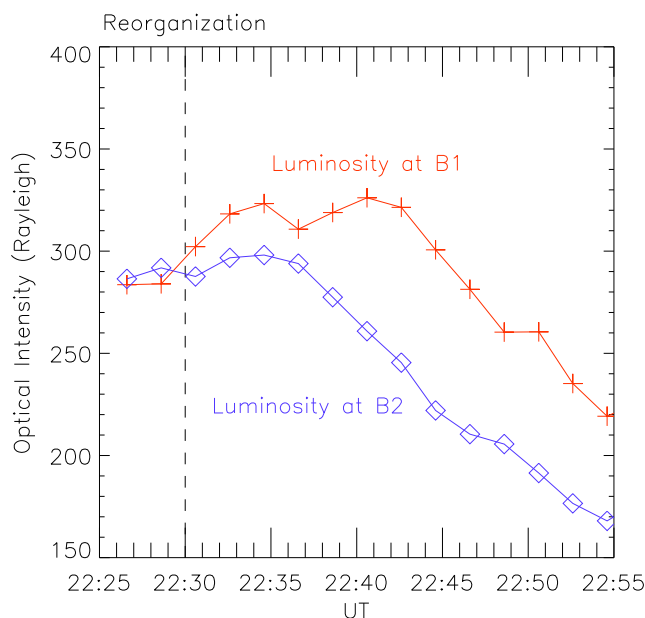
Figure 4. The 630.0 nm optical intensity at the centers of patches B1 (red) and B2 (blue), respectively.

vection pattern is more dependent on the actual radar data than on the model. However, the convection pattern sometimes changes drastically if we change the order of the spherical harmonics fitting. So, care must be taken when we choose the order of the fitting. The order of the spherical harmonics fitting used in the current analysis is 8. We generated convection maps with different orders of the fitting and examined how the change of the fitting order affects the convection pattern. Consequently, the convection map within the FOV of the imager did not change very much even if we employ a different order of the fitting. More importantly, the shear in the plasma flow near the gap between patches B1 and B2 can be seen even in the map with a different fitting order.

[14] We now briefly discuss the temporal evolution of the ionospheric convection during the 2 h period from 2130 to 2330 UT. The B_z component of the IMF divides this period into three intervals: 2130–2205 UT (interval I), 2205–2230 UT (interval II), and 2230–2330 UT (interval III). During interval I, the B_z component of the IMF was predominantly negative at around −5 nT, and strong anti-sunward flows were seen near the cusp throat region in the SuperDARN convection map (not shown). This is the time when the dayside equatorial magnetopause reconnection produced the patches and transported them deep into the central polar cap region. Interval II corresponds to a predominantly positive B_z period during which the convective flows at magnetic latitudes above 80° were quite weak (see Figures 3d and 3e). As shown in Figure 2, patch B almost stopped moving at 2218 UT and it stayed around the zenith of Resolute Bay until it was reorganized into two substructures. This behavior is consistent with the halt of the convection during this northward-oriented IMF interval. At 2230 UT, the IMF turned southward again, and the convection near patch B increased immediately. This is the time when the convection shear appeared and patch B started to

be reorganized into two substructures. This immediate response indicates that the B_z component of the IMF played an important role in the appearance of the velocity shear and the subsequent reorganization of patch B.

[15] While the IMF B_z maintained this orientation throughout interval III, the IMF B_y changed its direction at around 2250 UT. Before that time, B_y was almost stable at around 5 nT. Such an orientation of the IMF pulls the plasma convection near the dayside cusp inflow region dawnward. In contrast, the convection in the central polar cap region is directed duskward. This characteristic can be seen in most of the convection models such as *Ruohoniemi and Greenwald* [2005]. *Hosokawa et al.* [2009b] also showed that patches in the central polar cap drift duskward during an interval of positive IMF B_y. The observed convection direction in the central polar cap region after 2230 UT was due duskward, which was consistent with the orientation of the B_y and B_z components of the IMF at this time. We could not directly measure the convection pattern in the patches area after 2238 UT, since patches B1 and B2 stopped producing radar echoes. However, patches B1 and B2 drifted duskward after 2238 UT until they moved out of the FOV of the all-sky imager, which implies that the duskward plasma convection continued until the time of final image shown in Figure 2. This observation is consistent with the inference made about the convection model in the area, using observations from SuperDARN echoes in the vicinity (see equipotential contours in Figure 3).

[16] An important point to note is that the convection shear suddenly appeared at around 2230 UT when the IMF turned southward. It is not clear at this moment how this southward turning of the IMF affected the convection pattern near the cusp inflow region, because the spatial coverage of the radar data near the dayside cusp region was not good enough to examine the temporal evolution of the flow in relation to this change in IMF orientation. However, the correspondence between the appearance of the flow shear and the southward turning of the IMF indicates that the shear structure appeared when the convection pattern was reconfigured from the pre-existing northward-oriented IMF pattern to a twin-cell pattern after the southward turning of the IMF; thus, the change of the IMF B_z played a significant role in the reorganization of patch B.

[17] Another feature of interest is that the luminosity of the patches changed after the reorganization had occurred. Figure 4 shows the temporal variation of OI 630.0 nm optical emission at the centers of patches B1 and B2 (the centers of patches B1 and B2 are marked with a plus and a diamond in Figure 3, respectively) before and after the reorganization. The patch brightness observed by the all-sky imager depends on the zenith angle. So care must be taken when we extract the temporal variation of the luminosity of patch moving across the FOV of the imager. There are at least three factors affecting the luminosity of patches, (1) sensitivity decrease with increasing zenith angle, (2) so-called van Rhijn effect (increase in the volume per pixel with increasing zenith angle), and (3) atmospheric extinction. We carefully removed these effects by using the procedure introduced by *Kubota et al.* [2001]. Thus, the optical intensity shown in Figure 4 corresponds to the temporal variation of the patch luminosity. The optical intensity of both patches increased for 8−15 min after the
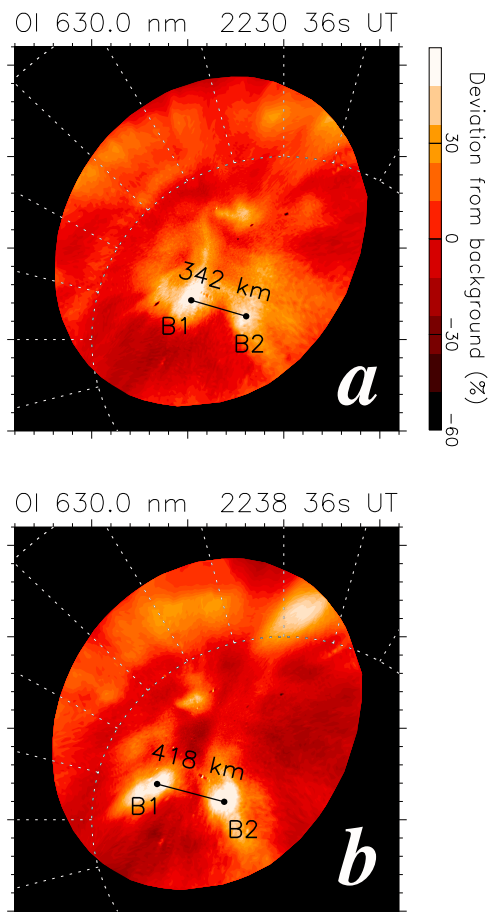
Figure 5. The 630 nm airglow images obtained at 2230 and 2238 UT, using which the distance between patches B1 and B2 is estimated.

start of reorganization. After a while, the luminosity started to decrease instead, until the end of the interval. This significant decay of patch luminosity is clearly seen in Figure 2 and is possibly associated with the duskward motion of patches. We will discuss this point in more detail in the next section.

4. Discussion and Conclusion

[18] The current observations of polar cap patches by simultaneous optical and radar measurements suggest that patches can be reorganized into smaller substructures due to a change in the background plasma convection field. It is clearly shown in Figure 3 that the reorganization of patch B occurred soon after a stalling in the convection, which was followed by the appearance of a shear in the convection velocities. Here, we qualitatively assess the correspondence between the reorganization of patch B and the shear in the convection velocity. Before proceeding, it should be noted that patch B already had mesoscale structures corresponding to patches B1 and B2 before it was reorganized into two substructures, which can be seen in the images recorded at 2228 and 2230 UT (Figures 3b and 3c). As shown in Figure 5a, the distance between the centers of these two mesoscale structures was approximately 342 km at 2230 UT.

After the appearance of the shear structure, patch B1 gradually moved away from patch B2, and then the distance between them became approximately 418 km (Figure 5b) at 2238 UT. Thus, the separation between the patches increased by approximately 80 km in 8 min.

[19] Figure 6 shows the temporal variation of the Super-DARN convection speed at the centers of patches B1 and B2. Note that the gray symbols on the line mean that the radar backscatter echoes were not directly available in the patches area itself; the speed was nevertheless inferred from the SuperDARN convection map. Figure 6 again demonstrates that the shear in the convection speed occurred at around 2230 UT when the B_z component of the IMF turned southward. This shear structure continued for at least 10 min, and the average difference in the convection speed at the centers of patches B1 and B2 was approximately 120 m s^{-1}. This velocity shear of approximately 120 m s^{-1}/ 340 km gives a distance of approximately 60 km. Given that we now know that SuperDARN convection speeds can be as small as three-fourth of the true plasma velocity at this time [*Gillies et al.*, 2009, and references therein], this value should be considered to be consistent with the increase in the distance estimated from Figure 5. This suggests that one of the causal factors of the reorganization of patch B was the velocity shear structure in its vicinity.

[20] The other possible factor causing the reorganization of the patch is a temporal change of the background convection due to the flipping of the IMF. *Sojka et al.* [1993] have suggested that simple flipping of the B_y component of the IMF can detach polar cap patches from TOI. This process may explain the reorganization of the patch plasma during the current interval. Actually, there existed many spiky changes in the IMF B_y before 2230 UT. These rapid changes in the IMF B_y probably chopped the
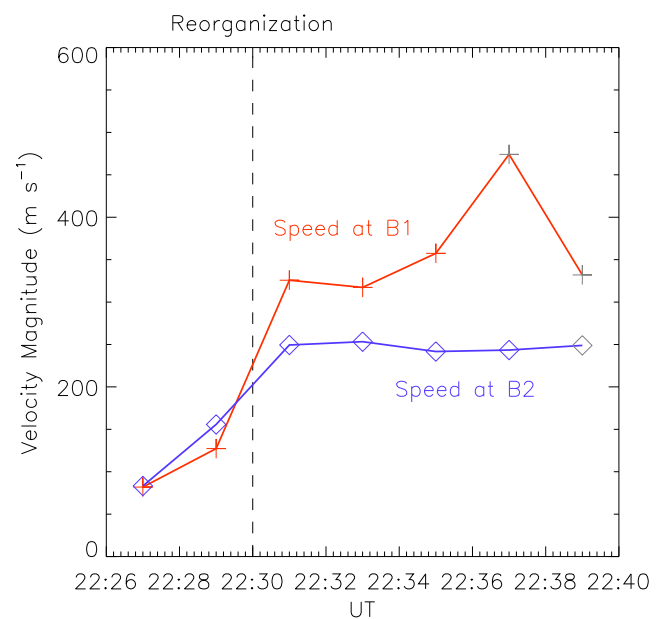

Figure 6. The convection speeds at patches B1 (red) and B2 (blue), respectively. The gray symbols on the line mean that the radar backscatter echoes were not available, and then the speed was inferred from the SuperDARN convection map.

tongue of ionization and produced patches near the dayside cusp inflow region. However, during the reorganization of patch B in the central polar cap (after 2230 UT), there was no outstanding changes in the IMF B_y (Figure 1a). This suggests that the reorganization of the patch structure starting at around 2230 UT was not directly associated with the temporal change of the IMF B_y but with the spatial shear in the background convection.
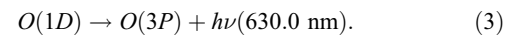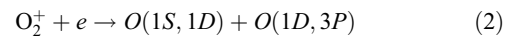
[21] The current observations suggest that a convection shear can contribute to the reorganization of patches in the central polar cap region. As mentioned in section 1, the deformation of patches into a so-called boundary blob in the nightside auroral region is also dominated by the spatial shear in the convection pattern in the equatorward part of the auroral zone [e.g., *Tsunoda*, 1988]. We can see some similarity between the reorganization of patch B in the central polar cap and the generation of blobs in the nightside because both of them are dominated by a shear in the background convection pattern. In Figure 3h, it is easy to infer that patches B1 and B2 straddle different convection streamlines having different plasma velocities. Convection near patch B1 originates from the high-speed flow observed on the dayside (red and orange vectors in Figure 3h), while that around patch B2 becomes part of the dawnside convection cell. This situation is quite similar to the convection pattern in the vicinity of boundary blobs on the nightside. This clearly indicates that the location of patch B was favorable for the reorganization into two substructures through the convection shear.

[22] However, there exists a big difference between boundary blobs and the current polar cap patch in terms of the spatial structure. That is, the patch in the current observation was clearly reorganized into two substructures while boundary blobs are only elongated. We need to address why we observed reorganization instead of an elongation. One possible way to explain this is that the ion density in the middle of patch B became too small to produce enough luminosity to be detected by the airglow imager. Such a reduction in the optical intensity at the gap could quicken the rate of reorganization, causing the patch to be reorganized into two substructures. We now discuss a process through which the luminosity in the middle of patch B could have decreased.

[23] If we consider the ion continuity equation, the ion density in the frame moving with the background flow is affected by a divergence of the flow in the electric field direction (i.e., Pedersen direction). That is, a divergence of the ions through Pedersen currents can decrease the density of the patch while a convergence can increase it. If we examine the 2-D flow pattern near the gap between patches B1 and B2 shown in Figure 3h, there is an apparent steady increase in the duskward flow as we go sunward. This means that there is a weak increase in the electric field in the electric field direction, which is sunward in this case. This produces a small divergence in the electric field corresponding to a divergence in the Pedersen currents carried mainly by ions. The divergence in the electric field is most apparent at the gap between patches B1 and B2. This divergence can decrease the ion density in the middle of patch B; thus, it can contribute to the reorganization of patch B into two individual parts. This being stated, however, the divergence in the Pedersen currents appears

too weak to compete with chemical processes. This can be seen by comparing the Pedersen divergence term $n_i(\nu_i/\Omega_i)\nabla \cdot (\mathbf{E}/B)$ with the chemical loss term, which is of the order of $6 \times 10^{-4} n_i$. Using $\nu_i/\Omega_i \approx 10^{-1}$ and $\nabla \cdot (\mathbf{E}/B) \approx 120$ m s^{-1}/340 km, we obtain approximately $-3.5 \times 10^{-5} n_i$ from the Pedersen divergence term, i.e., more than one order of magnitude less than the chemical recombination term. This term is therefore not competitive unless the divergence in the electric field operates on a much smaller scale than 340 km.

[24] This brings us to another process that is potentially more important and is associated with chemistry. As shown in Figure 4, the luminosity of patches B1 and B2 showed a very unique behavior after the reorganization. Namely, after the reorganization, the luminosity at first increased. After that, the luminosity decreased steadily and finally fell back to the background level (i.e., the patch cease to exist). Since patches B1 and B2 were traveling in the dark hemisphere far away from the source region near the cusp, there should have been no ion chemical production. Thus, the luminosity of patch had to increase through a process other than photoionization. One thing we have to bear in mind is that the luminosity started increasing soon after the reorganization, which coincided with the onset of duskward convection in the vicinity of the patch. This suggests that the change in patch motion had something to do with the luminosity change. Indeed, during the interval of duskward convection, the plasma within the patch was moving away from the magnetic pole, which means that the $\mathbf{E} \times \mathbf{B}$ drift had a small downward component. Here, we intend to interpret the luminosity change in terms of vertical motion of the patch. The OI 630.0 nm optical emission associated with patches comes from the following chemistry:

$$O^+ + O_2 \rightarrow O_2^+ + O \tag{1}$$

$$O_2^+ + e \rightarrow O(1S, 1D) + O(1D, 3P) \tag{2}$$

$$O(1D) \rightarrow O(3P) + h\nu(630.0 \text{ nm}). \tag{3}$$

The production of the molecular oxygen ion through dissociative recombination, equation (1), determines the efficiency of the whole process because the timescale of this process is much longer than that of others. As the plasma moves downward, the rate at which O_2^+ ions are produced goes up at first because of the larger O_2 densities at lower altitudes. This in turn results in an increase in the 630.0 nm emission rate through equations (2) and (3). However, the more O_2^+ and NO^+ ions are produced as the patch moves down, the fewer O^+ ions there are. Ultimately, this leads to a decrease in the patch density, and in the red line emissions themselves. While it is beyond the scope of this paper to delve into the details of this mechanism (a separate manuscript is currently in preparation), we do note here that with their different speeds, patches B1 and B2 will evolve a very different brightness and, with it, a very difference density, to the point that they will ultimately become separate entities. This might explain why the initial patch B ultimately broke into two distinct patches instead of

just continuing to elongate as it would have done near the edge of the polar cap at more equatorward latitudes. In the latter case, the circulation is roughly along a circle of magnetic latitude and is therefore basically devoid of the vertical motion that causes the breakup that occurs when the circulation is across circles of magnetic latitude and sheared.

[25] In summary, we introduced a case in which polar cap patch was reorganized into substructures possibly in association with a shear in the background convection pattern. We investigated the divergence associated with Pedersen drifts as a possible contributor to the reorganization of the patch. Our estimates led us to the conclusion that this contribution was less important than chemistry. The latter could, however, lead to a breakup into separate patches in the presence of shears because of the differences in recombination rates associated with different rates of descent. No matter what the final word on the subject may be, our observations clearly indicate that a mesoscale structure in the plasma convection in the central polar cap area is one of the important factors controlling the behavior of patches.

[26] Recently, *Hosokawa et al.* [2009a] have conducted simultaneous observations of patches and patch-associated field-aligned irregularities (FAIs) in the central polar cap region. They showed that the FAIs were found to extend over the entire region of enhanced airglow associated with polar cap patches, indicating that the plasma patches became almost fully structured soon after their initiation (within approximately 20–25 min). Such kind of fast structuring process could not be explained only by the plasma stirring through gradient drift instability. Thus, some other process could be involved in addition to the primary gradient drift instabilities. On the basis of the current observations, we suggest here that the reconfiguration/deformation of patches because of a shear in the background convection field may well play an important role in the rapid structuring of patches simply by reorganizing large patches into a number of smaller substructures.

References

Anderson, D. N., J. Buchau, and R. A. Heelis (1988), Origin of density enhancements in the winter polar cap ionosphere, *Radio Sci.*, 23, 513–519.

Baker, K. B., and S. Wing (1989), A new magnetic coordinate system for conjugate studies of high latitudes, *J. Geophys. Res.*, 94, 9139–9143.

Carlson, H. C., J. Moen, K. Oksavik, C. P. Nielsen, I. W. McCrea, T. R. Pedersen, and P. Gallop (2006), Direct observations of injection events of subauroral plasma into the polar cap, *Geophys. Res. Lett.*, 33, L05103, doi:10.1029/2005GL025230.

Chisham, G., et al. (2007), A decade of the Super Dual Auroral Radar Network (SuperDARN): Scientific achievements, new techniques and future directions, *Surv. Geophys.*, 28, 33–109, doi:10.1007/s10712-007-9017-8.

Crowley, G. (1996), Critical review of ionospheric patches and blobs, in *Review of Radio Science 1993–1996*, edited by W. R. Stone, pp. 619–648, Oxford Univ. Press, New York.

Decker, D., C. Valladares, R. Sheehan, S. Basu, D. Anderson, and R. Heelis (1994), Modeling daytime F layer patches over Sondrestrom, *Radio Sci.*, 29, 249–268.

de la Beaujardiere, O., and R. A. Heelis (1984), Velocity spike at the poleward edge of the auroral zone, *J. Geophys. Res.*, 89, 1627–1634.

Gillies, R. G., G. C. Hussey, G. J. Sofko, K. A. McWilliams, R. D. Fiori, P. Ponomarenko, and J. P. St.-Maurice (2009), Improvement of SuperDARN velocity measurements by estimating the index of refraction in the scattering region using interferometry, *J. Geophys. Res.*, 114, A07305, doi:10.1029/2008JA013967.

Greenwald, R. A., et al. (1995), DARN/SuperDARN: A global view of the dynamics of high-latitude convection, *Space Sci. Rev.*, 71, 761–796.

Heelis, R., J. Lowell, and R. Spiro (1982), A model of the high-latitude ionospheric convection pattern, *J. Geophys. Res.*, 87, 6339–6345.

Hosokawa, K., K. Shiokawa, Y. Otsuka, A. Nakajima, T. Ogawa, and J. D. Kelly (2006), Estimating drift velocity of polar cap patches with all-sky airglow imager at Resolute Bay, Canada, *Geophys. Res. Lett.*, 33, L15111, doi:10.1029/2006GL026916.

Hosokawa, K., K. Shiokawa, Y. Otsuka, T. Ogawa, J.-P. St-Maurice, G. J. Sofko, and D. A. Andre (2009a), Relationship between polar cap patches and field-aligned irregularities as observed with an all-sky airglow imager at Resolute Bay and the PolarDARN radar at Rankin Inlet, *J. Geophys. Res.*, 114, A03306, doi:10.1029/2008JA013707.

Hosokawa, K., T. Kashimoto, S. Suzuki, K. Shiokawa, Y. Otsuka, and T. Ogawa (2009b), Motion of polar cap patches: A statistical study with all-sky airglow imager at Resolute Bay, Canada, *J. Geophys. Res.*, 114, A04318, doi:10.1029/2008JA014020.

Hosokawa, K., T. Tsugawa, K. Shiokawa, T. Otsuka, T. Ogawa, and M. Hairston (2009c), Unusually elongated bright optical plume in the polar cap F region: Is it a tongue of ionization?, *Geophys. Res. Lett.*, 36, L07103, doi:10.1029/2009GL037512.

Khan, H., and S. W. H. Cowley (1999), Observations of the response time of high-latitude ionospheric convection to variations in the interplanetary magnetic field using EISCAT and IMP-8 data, *Ann. Geophys.*, 17, 1306–1335.

Koustov, S. A., K. Hosokawa, N. Nishitani, T. Ogawa, and K. Shiokawa (2008), Rankin Inlet PolarDARN radar observations of duskward moving Sun-aligned optical forms, *Ann. Geophys.*, 26, 2711–2723.

Knudsen, W. C. (1974), Magnetospheric convection and the high-latitude F2 ionosphere, *J. Geophys. Res.*, 79, 1046–1055.

Kubota, M., H. Fukunishi, and S. Okano (2001), Characteristics of medium- and large-scale TIDs over Japan derived from OI 630-nm nightglow observation, *Earth Planets Space*, 53, 741–751.

Lockwood, M., and H. C. Carlson Jr. (1992), Production of polar cap electron density patches by transient magnetopause reconnection, *Geophys. Res. Lett.*, 19, 1731–1734.

Lorentzen, D. A., N. Shumilov, and J. Moen (2004), Drifting airglow patches in relation to tail reconnection, *Geophys. Res. Lett.*, 31, L02806, doi:10.1029/2003GL017785.

Milan, S. E., M. Lester, and T. K. Yeoman (2002), HF radar polar patch formation revisited: Summer and winter variations in dayside plasma structuring, *Ann. Geophys.*, 20, 487–499.

Moen, J., H. C. Carlson, K. Oksavik, C. P. Nielsen, S. E. Pryse, H. R. Middleton, I. W. McCrea, and P. Gallop (2006), EISCAT observations of plasma patches at sub-auroral cusp latitudes, *Ann. Geophys.*, 24, 2363–2374.

Ogawa, T., S. C. Buchert, N. Nishitani, N. Sato, and M. Lester (2001), Plasma density suppression process around the cusp revealed by simultaneous CUTLASS and EISCAT Svalbard radar observations, *J. Geophys. Res.*, 106, 5551–5564.

Ridley, A. J. (2000), Estimations of the uncertainty in timing the relationship between magnetospheric and solar wind processes, *J. Atmos. Sol. Terr. Phys.*, 62, 757–771.

Robinson, R. M., R. T. Tsunoda, J. F. Vickrey, and L. Guerin (1985), Sources of F region ionization enhancements in the nighttime auroral zone, *J. Geophys. Res.*, 90, 7533–7546.

Rodger, A. S., M. Pinnock, J. R. Dudeney, K. B. Baker, and R. A. Greenwald (1994), A new mechanism for polar patch formation, *J. Geophys. Res.*, 99, 6425–6436.

Ruohoniemi, J. M., and K. B. Baker (1998), Response of high latitude convection to a sudden southward IMF turning, *Geophys. Res. Lett.*, 25, 2913–2916.

Ruohoniemi, J. M., and R. A. Greenwald (2005), Dependencies of high-latitude plasma convection: Consideration of interplanetary magnetic field, seasonal, and universal time factors in statistical patterns, *J. Geophys. Res.*, *110*, A09204, doi:10.1029/2004JA010815.

Shiokawa, K., Y. Katoh, M. Satoh, M. K. Ejiri, T. Ogawa, T. Nakamura, T. Tsuda, and R. H. Wiens (1999), Development of optical mesosphere thermosphere imagers (OMTI), *Earth Planets Space*, *51*, 887–896.

Shiokawa, K., Y. Katoh, M. Satoh, M. K. Ejiri, and T. Ogawa (2000), Integrating-sphere calibration of all-sky cameras for nightglow measurements, *Adv. Space Res.*, *26*, 1025–1028.

Shiokawa, K., Y. Otsuka, and T. Ogawa (2009), Propagation characteristics of nighttime mesospheric and thermospheric waves observed by optical mesosphere thermosphere imagers at middle and low latitudes, *Earth Planets Space*, *61*, 479–491.

Sojka, J. J., M. D. Bowline, R. W. Schunk, D. T. Decker, C. E. Valladares, R. Sheehan, D. A. Anderson, and R. A. Heelis (1993), Modeling polar cap F-region patches using time varying convection, *Geophys. Res. Lett.*, *20*, 1783–1786.

Suzuki, S., K. Shiokawa, K. Hosokawa, K. Nakamura, and W. K. Hocking (2009), Statistical characteristics of polar cap mesospheric gravity waves observed by an all-sky airglow imager at Resolute Bay, Canada, *J. Geophys. Res.*, *114*, A01311, doi:10.1029/2008JA013652.

Tsunoda, R. T. (1988), High latitude F region irregularities: A review and synthesis, *Rev. Geophys.*, *26*, 719–760.

Valladares, C., H. Carlson Jr., and K. Fukui (1994), Interplanetary magnetic field dependency of stable sun-aligned polar cap arcs, *J. Geophys. Res.*, *99*, 6247–6272.

Weber, E. J., J. Buchau, J. G. Moore, J. R. Sharber, R. C. Livingston, J. D. Winningham, and B. W. Reinisch (1984), F layer ionization patches in the polar caps, *J. Geophys. Res.*, *89*, 1683–1696.

K. Hosokawa, Department of Information and Communication Engineering, University of Electro-Communications, Chofugaoka 1-5-1, Chofu, Tokyo 182-8585, Japan. (hosokawa@ice.uec.ac.jp)

T. Ogawa, National Institute of Information and Communications Technology, Nukui-Kitamachi 4-2-1, Koganei, Tokyo 184-8795, Japan. (taogawa@nict.go.jp)

Y. Otsuka and K. Shiokawa, Solar-Terrestrial Environment Laboratory, Nagoya University, Nagoya, Aichi, Japan Furo-cho, Chikusa-ku, Nagoya 464-8601, Japan. (otsuka@stelab.nagoya-u.ac.jp; shiokawa@stelab.nagoya-u.ac.jp)

G. J. Sofko and J.-P. St-Maurice, Institute for Space and Atmospheric Studies, Department of Physics and Engineering Physics, University of Saskatchewan, 116 Science Place, Saskatoon, SK S7N 5E2, Canada. (george.sofko@usask.ca; jp.stmaurice@usask.ca)